phys. stat. sol. (b) **195**, 311 (1996)

Subject classification: 78.55; S10

Institute of Physics, Prague[1]) *(a), CERN, Division PPE, Geneve (b), Institute of Crystal Growth, Berlin*[2]) *(c), and IROE del CNR, Firenze*[3]) *(d)*

Slow Components in the Photoluminescence and Scintillation Decays of $PbWO_4$ Single Crystals

By

M. NIKL (a), K. NITSCH (a), K. POLAK (a), E. MIHOKOVA (a), I. DAFINEI (b), E. AUFFRAY (b), P. LECOQ (b), P. REICHE (c), R. UECKER (c), and G. P. PAZZI (d)

(Received December 22, 1995)

The decay kinetics of $PbWO_4$ luminescence and scintillation is investigated in a broad time scale 10^{-9} to 10^{-3} s mainly at room temperature using a selected set of $PbWO_4$ crystals. The light sum released in different time gates is estimated showing rather high content of slow recombination processes related mainly to the green $PbWO_4$ emission component. Correlations are found among the absolute green emission intensity, crystal light yield, and the amplitude of very slow processes in the $PbWO_4$ scintillation decay.

Das Abklingen der Lumineszenz und der Scintillation von $PbWO_4$ wird in einem breiten Zeitbereich von 10^{-9} bis 10^{-3} s vor allem bei Zimmertemperatur untersucht. Die in verschiedenen Zeitspannen entstehende Lichtsumme wird abgeschätzt, und es wird gezeigt, daß sie einen hohen Gehalt von langsamen Rekombinationsprozessen umfaßt, die vor allem auf die grüne Lumineszenzkomponente bezogen ist. Es wird eine Korrelation zwischen der wirklichen Intensität der grünen Emission, dem Kristallichtertrag und der Amplitude der langsamen Prozesse des Scintillationsabklingens von $PbWO_4$ gefunden.

1. Introduction

Luminescence of $PbWO_4$ (PWO) was investigated in the past by several authors [1 to 3]. At present, there is again an increased interest in the optical and especially in the scintillation properties of this material, as PWO was found to satisfy the requirements for fast scintillation detectors in the GeV and TeV energy range in high energy physics [4, 5]. Furthermore, PWO was recently approved as scintillating material for the electromagnetic calorimeter (ECAL) in the Large Hadron Calorimeter (LHC) project in CERN. Its high density ($\varrho = 8.28$ g/cm^3) is the main advantage comparing to previously favoured material – CeF_3 [6], because PWO enables to reduce the volume of the calorimeter detector (about twice with respect to CeF_3), which means a strong reduction in price as well.

Photoluminescence (PL) of PWO is composed of two components – the blue one peaking about 410 to 420 nm and the green one at 480 to 520 nm. The blue emission was ascribed to the regular WO_4 group [1], while the green one is related to the defect

[1]) Cukrovarnicka 10, 16200 Prague, Czech Republic.
[2]) Rudower Chaussee 6, D-12489 Berlin, Federal Republic of Germany.
[3]) Via Paneiatichi 64, I-50-127 Firenze, Italy.

WO_3 group [2], possibly with F centre nearby [7]. Also red emission of PWO is reported [7], which is ascribed to Pb^{3+} and depends strongly on the purity and stoichiometry of the starting material and the growth technology. PL decay kinetics [1] shows rather complicated nonmonotonic temperature dependence of decay times in both blue and green PWO emission components.

The scintillation spectrum at room temperature (RT) under γ (Na^{22} isotope, 511 keV photons) or X-ray excitations shows also both blue and green emission components [5, 7]. The scintillation decay measured within 500 ns TAC time gate at RT was approximated by the sum of three exponentials showing the decay times $\tau_1 = 5.1$ ns, $\tau_2 = 14$ ns, and $\tau_3 = 110$ ns [7].

Very recently it was shown that apart from ns decay components, much slower processes appear in PWO decay both under selective band-to-band UV and 511 keV γ excitations [8, 9] and that these processes are related mainly to the green PWO emission component. Furthermore, pronounced differences were found in the shapes of the emission spectra of PWO grown by different producers [8].

Using a selected set of PWO single crystal samples, it is the aim of this paper to evidence the general occurrence of so-called "superslow" components in the scintillation decay of PWO and to show that correlations exist among the steady-state scintillation emission spectra shapes (and intensity), the amplitude of the superslow components in the scintillation decay, and also the light yield (LY) of the PWO crystals studied. As the amount of light extracted from the PWO scintillator within the first 100 ns is most important for LHC application, an estimate of the contribution of fast (0 to 100 ns) and slow (>100 ns) processes to the PWO photoluminescence decay is calculated and a similar parameter is roughly estimated from the scintillation decays, too.

2. Experimental Methods and Sample Preparation

UV and X-ray excited steady-state spectra and PL decays were measured at the modified spectrofluorometer 199S [10], scintillation decays were measured using the radioisotope ^{22}Na and the classical coincidence method [11]. PWO decay under laser excitation was measured using a LISS-Multilaser, model 780U excimer laser with nitrogen–helium mixture ($E_{\max}^{\text{puls}} \doteq 1$ mJ, $\lambda_{\text{em}} \doteq 337.1$ nm, FWHM $\doteq 7$ ns) with a Hamamatsu R1398 photomultiplier (PMT) detection coupled to the Tektronix 2440 digital memory oscilloscope. All the spectra are corrected for the set-up spectra characteristics and a deconvolution procedure is applied to the decay curves in ns time scale to remove the instrumental response influence and to obtain the true decay times. LY measurements were performed with a Co radioisotope measuring in ac mode the photopeak position with MCHA registration and 1 μs shaping time.

Recent PWO samples grown by the Czochralski method were used for the measurements, namely: PWO grown by Bogoroditsk Technicochemical Plant, Russia (No. 1168, 1174, 1181), by Shanghai Institute of Ceramics, China (No. 1180, Bridgman grown), and by K. Nitsch in collaboration with the Institute of Crystal Growth, Germany (No. 1185). More detailed description of the growth technology is given in [7] as for Russian samples which were grown from typically 4N raw materials. At least 5N PbO and grade A1 WO_3 (6 ppm of total metallic impurities) were used in the case of PWO 1185, the detailed description of the growth procedure is given elsewhere [12]. 3N WO_3 and 4N PbO materials were used in the case of PWO 1180, more details are given in [13].

3. Experimental Results

The blue and green PWO emission components (Fig. 1, curves d, e) can be well resolved at 4.2 K using selective UV excitation enabled by the different excitation spectra, Fig. 1, curves a, c. The excitation peak at 295 nm (4.2 K) broadens and moves to lower energies with increasing temperature (Fig. 1, curve b). On the contrary, the excitation peak of the green emission at about 310 nm only little depends on temperature. At RT, the excitation spectra of both spectral components are very similar. Using the knowledge from PL as to shape and position of the blue and green component spectra, a consistent decomposition of X-ray excited steady-state PWO emission was made in the 80 to 300 K temperature interval (inset of Fig. 2) showing strong quenching of both components at RT. The mutual intensity ratio between the blue and green components is strongly sample dependent, see Fig. 2. The steady-state emission spectra in Fig. 2 are measured under the same experimental conditions and with samples of similar shape (typically plates about $8 \times 10 \times 2\ mm^3$), so that they can be mutually compared also in absolute scale as done in Fig. 3, i.e. they can serve to obtain information about the steady-state LY.

The temperature dependence of the PL decay times is given in Fig. 4. While at the lowest temperatures both emission components show a single exponential decay, a slower tail appears in the green emission decay above 180 K even under 313 nm excitation, which is actually in the PWO band edge well below the band-to-band transition (green emission decay times above 180 K are obtained using a single exponential fit of

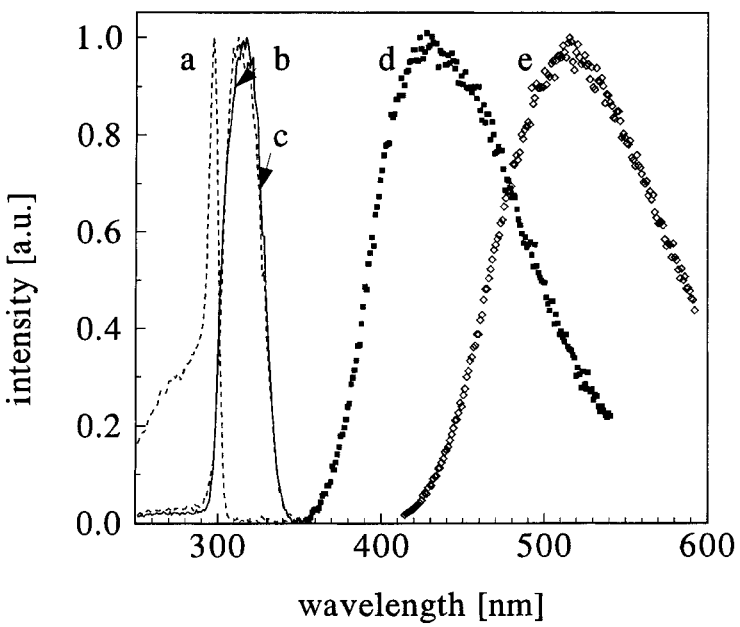

Fig. 1. Excitation (curves a, b, c) and emission (curves d, e) spectra of PWO crystal (sample independent). (a) $\lambda_{em} = 400$ nm, $T = 4.2$ K; (b) $\lambda_{em} = 400$ nm, $T = 295$ K (solid line); (c) $\lambda_{em} = 560$ nm, $T = 4.2$ K (dashed line); (d) $\lambda_{exc} = 290$ nm, $T = 4.2$ K; (e) $\lambda_{exc} = 315$ nm, $T = 4.2$ K (a.u. means arb.units)

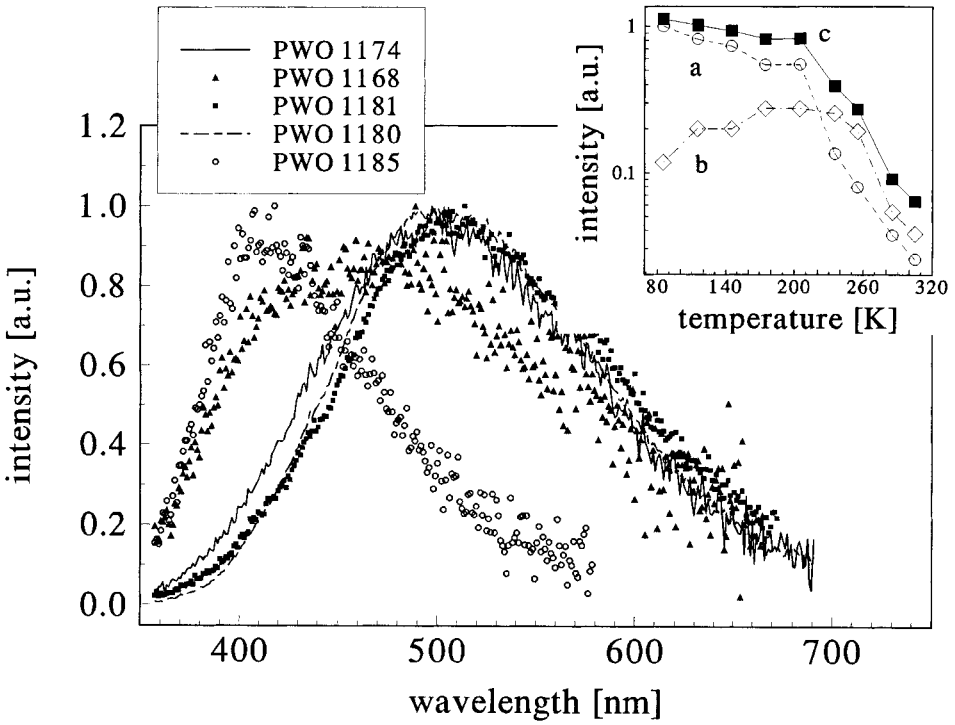

Fig. 2. X-ray excited steady-state emission spectra of PWO crystals at 295 K. All spectra are normalized to unity. In the inset, the temperature dependence of steady-state X-ray excited PWO emission is given, (a) blue and (b) green components, (c) overall emission intensity

the initial part of the decay curve). An example of the blue and green emission decays at 220 K is given in Fig. 5. The effect of the increased background level with respect to the true dark PMT count rate in the green component decay was noticed (Fig. 5b) – the level appropriate to the dark photomultiplier (PMT) counts was considered in the decay approximation by a solid line. Apart from the effect described below in Fig. 9, also uncorrelated thermostimulated luminescence (TSL) could increase the background level, because the TSL peak was reported at 216 K [14] and these decay measurements were made at a single temperature run starting from 80 K and even higher background level was observed in the decay measurement at 200 K.

Furthermore PL decay was measured under UV band-to-band excitation at 230 nm using an intense xenon μs-pulse flashlamp (FWHM = 2 μs, 0.2 J/pulse) for the excitation to reveal the time dependence of the radiative processes involving free carrier recombination. It comes out that in both spectral components of PWO emission very slow components are present as well, and an example of the decay is given in Fig. 6. The mean decay time

$$\tau_{\mathrm{m}} = \frac{\int tI(t)\,\mathrm{d}t}{\int I(t)\,\mathrm{d}t} \tag{1}$$

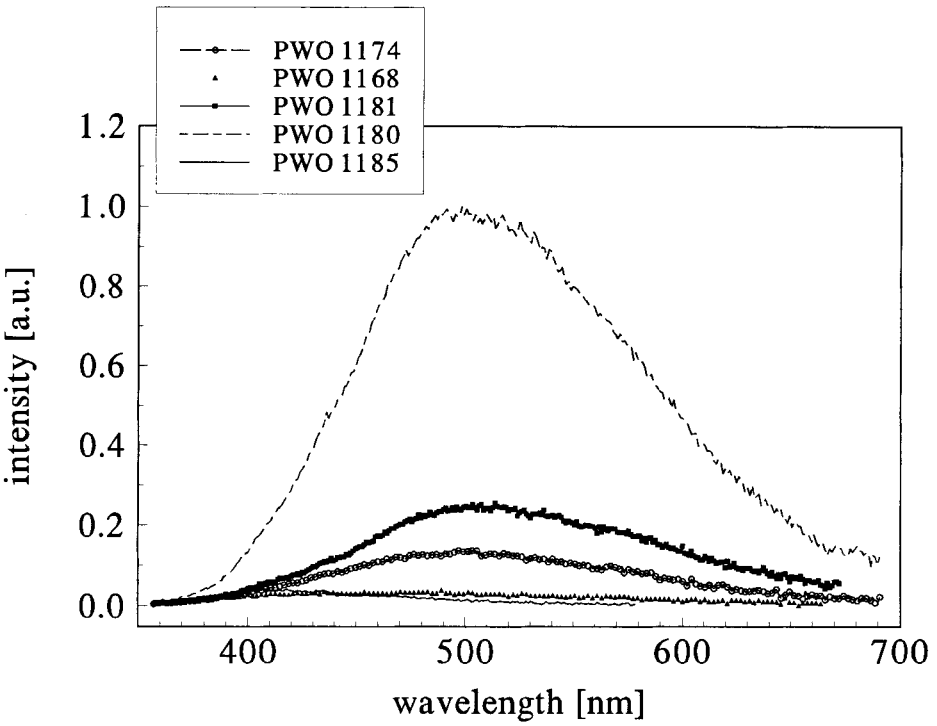

Fig. 3. X-ray excited steady-state emission spectra of PWO crystals at 295 K. The spectra are given in absolute scale (i.e. the intensities are mutually comparable)

can be calculated for different PWO crystals at RT showing values $\tau_m \in \langle 0.59, 0.99 \rangle$ ms at $\lambda_{em} = 400$ nm and $\langle 1.22, 1.89 \rangle$ ms at $\lambda_{em} = 500$ nm. Using the advantage of a low repetition rate (about 2 Hz) of the excitation produced by the ns intense N_2-laser line and very fast PMT detection in the bias regime, PWO 1180 decay at 500 nm (and the spectral width of 30 nm) was measured at RT in different time scales and oscilloscope sensitivities under otherwise the same experimental conditions. Pasting the decay curves enables to obtain the decay through as much as six orders of magnitude in time and about four orders of dynamic range, Fig. 7. By the integration of the decay curve in the time gates (10^{-9} to 10^{-7}) s (fast component I_f) and (10^{-7} to 10^{-3}) s (slow component I_s), the estimate of the amount of light released in these two time gates can be obtained, namely

$$I_f \doteq 1.0 \times 10^{-8}, \qquad I_s \doteq 66 \times 10^{-8}, \tag{2}$$

i.e. $I_f \doteq 1.5\%$ of the overall emission intensity within the conditions given for this particular measurement. The time gate $\langle 0, 100 \rangle$ ns was chosen according to the expected time gate to be used in the LHC experiment. Furthermore, it was found that the relative amplitude of the decay tail (time gate 400 ns) is strongly dependent on the excitation intensity, Fig. 8.

An example of a PWO 1180 scintillation decay is given in Fig. 9 (curve a). The decay is fitted by the sum of three exponentials convoluted with the instrumental response and

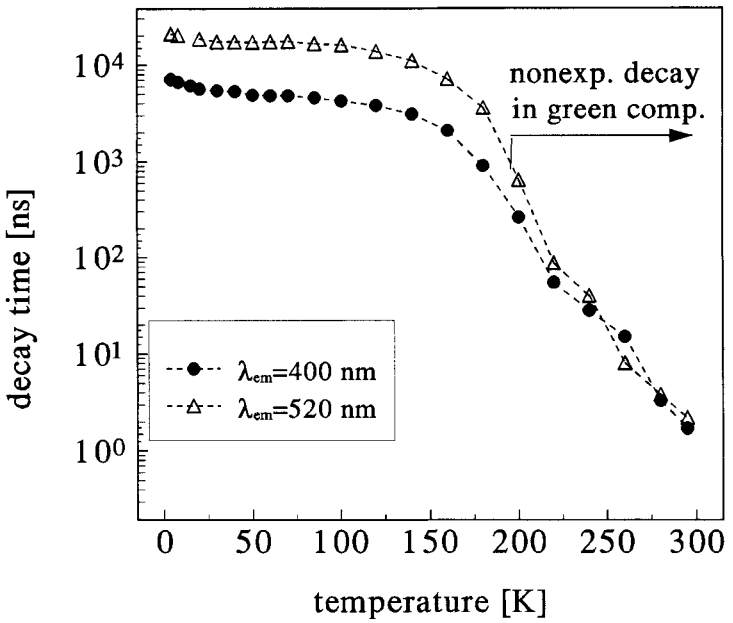

Fig. 4. Temperature dependence of the PL decay times of the blue ($\lambda_{em} = 400$ nm) and green ($\lambda_{em} = 520$ nm) components (PWO 1174). The excitation wavelengths were chosen at any temperature near the maxima of excitation spectra ($\lambda_{exc}^{400\,nm} = 295$ to 310 nm, $\lambda_{exc}^{520\,nm} = 310$ nm)

calculating the background level from the signal before the rising edge of the decay pulse. However, as was already noticed [8], the amplitude of the signal in a PWO scintillation decay measurement preceding the rising edge of the decay iself, is higher than that expected from the dark photomultiplier (PMT) count rate. So-called "no crystal" decay is given in Fig. 9, curve b (measured at the same experimental conditions, accumulation time, etc., but without the PWO sample). The "no crystal" decay shows the true background level valid for the displayed PWO decay curve. The sharp peak caused by the direct interaction of γ-quanta with PMT can be taken as the instrumental response of the set-up to a δ-excitation. The mentioned increased amplitude of the signal preceding the decay pulse can be thus explained only by the existence of decay processes slow in comparison with the average excitation rate of the sample, i.e. repetition rate of

Table 1

The coefficient α derived from scintillation decay measured at $\lambda_{em} = 400$ nm, 500 nm and spectrally unresolved, light sum in the superslow component IS_s and the light yield LY for the set of PWO crystals; $T = 295$ K

sample	α (400 nm) [%]	α (500 nm) [%]	α (unres.) [%]	IS_s [%]	LY [phot./MeV]
PWO 1168	0.63	1.86	1.1	98.9	171
PWO 1174	0.84	4.5	2.0	99.2	214
PWO 1180	0.94	8.5	3.5	99.6	378
PWO 1181	0.44	4.1	1.8	99.5	not meas.
PWO 1185	not meas.	not meas.	0.85	98.7	153

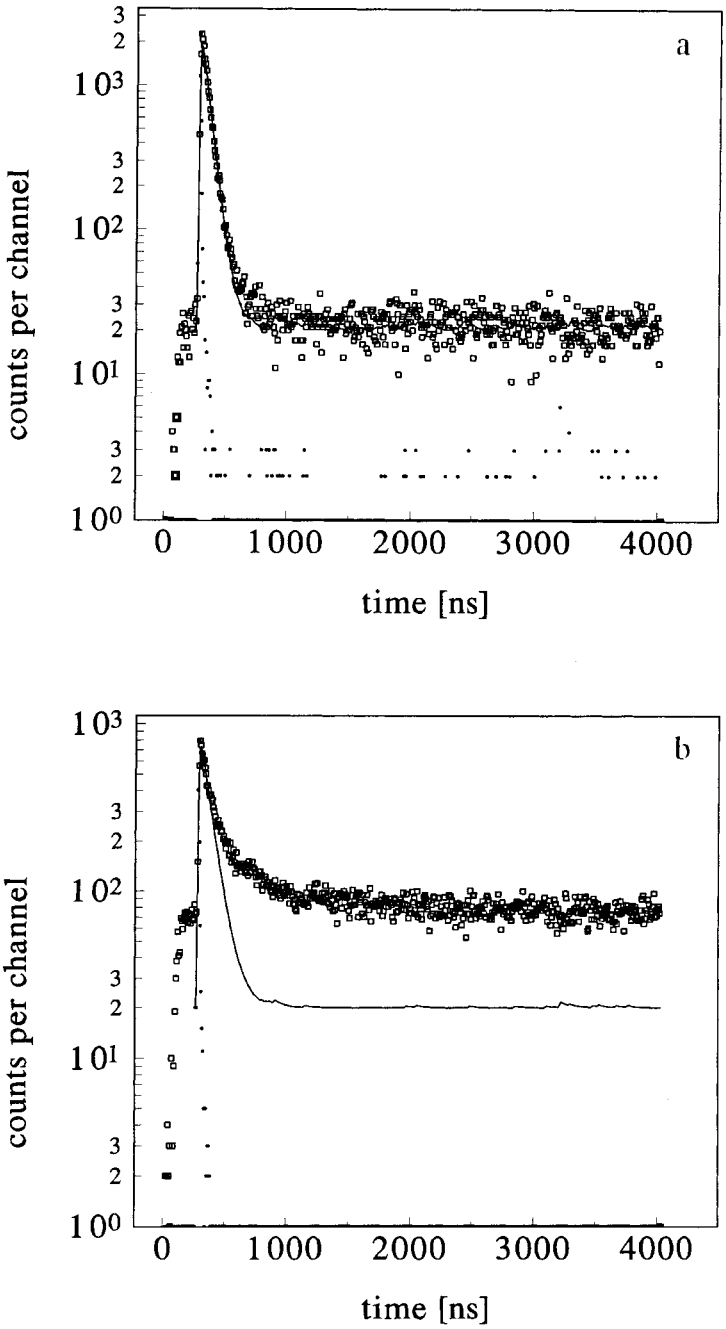

Fig. 5. PL decay of the a) blue and b) green components of PWO 1174 at 220 K. a) $\lambda_{exc} = 300$ nm, $\lambda_{em} = 400$ nm; b) $\lambda_{exc} = 313$ nm, $\lambda_{em} = 520$ nm. Convolution of instrumental response (indicated in the figure by smaller dots) with single exponential approximations are given by the solid lines showing decay times of 58 and 84 ns, respectively. The true background level determined only by dark PMT counts is considered in the fits

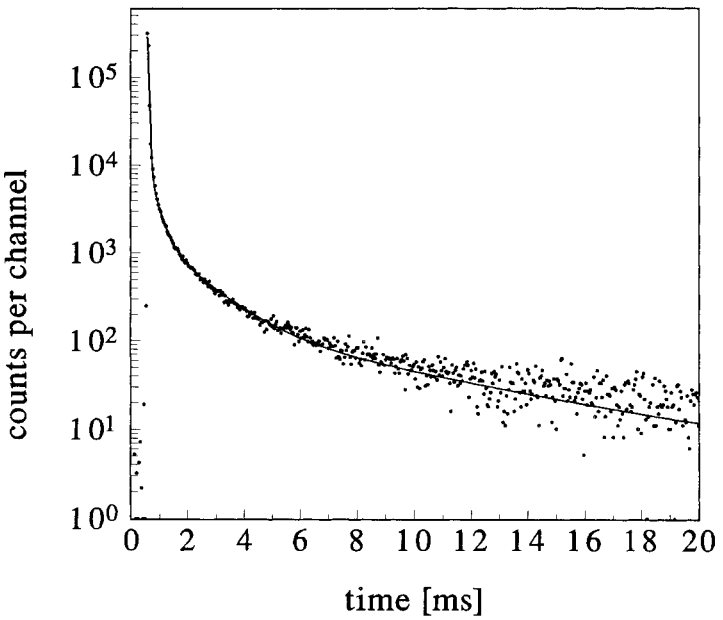

Fig. 6. PL decay of the blue component of PWO 1185 under band-to-band UV excitation at RT, $\lambda_{exc} = 230$ nm, $\lambda_{em} = 400$ nm. Four exponential approximations are given by the solid line with relative pre-exponential factors A_i and decay times τ_i: $A_1 = 4.5$, $\tau_1 = 0.035$ ms; $A_2 = 0.073$, $\tau_2 = 0.284$ ms; $A_3 = 0.018$, $\tau_3 = 1.38$ ms; $A_4 = 0.0014$, $\tau_4 = 6.6$ ms

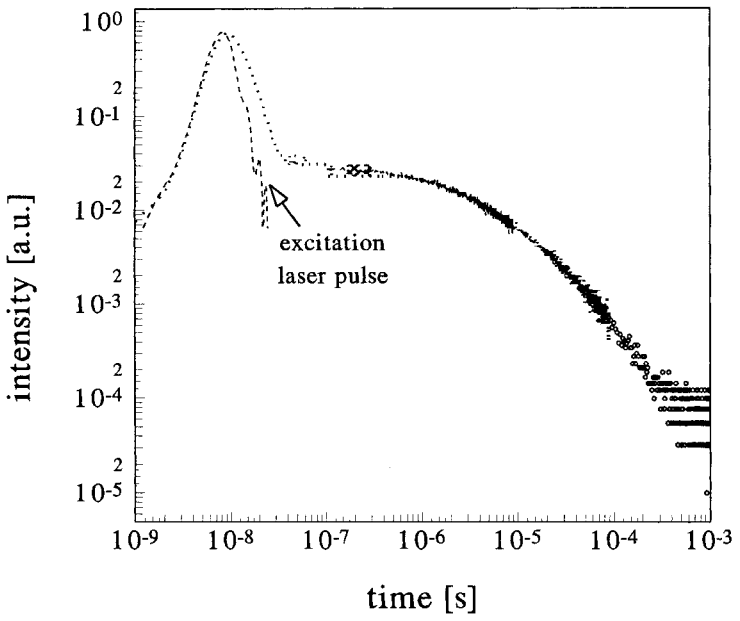

Fig. 7. N_2-laser line (337.1 nm, $E_{puls} = 1$ mJ) excited PL decay of PWO 1180 at RT and $\lambda_{em} = 500$ nm showing at the same time fast and slow components of the decay (for the construction see the text)

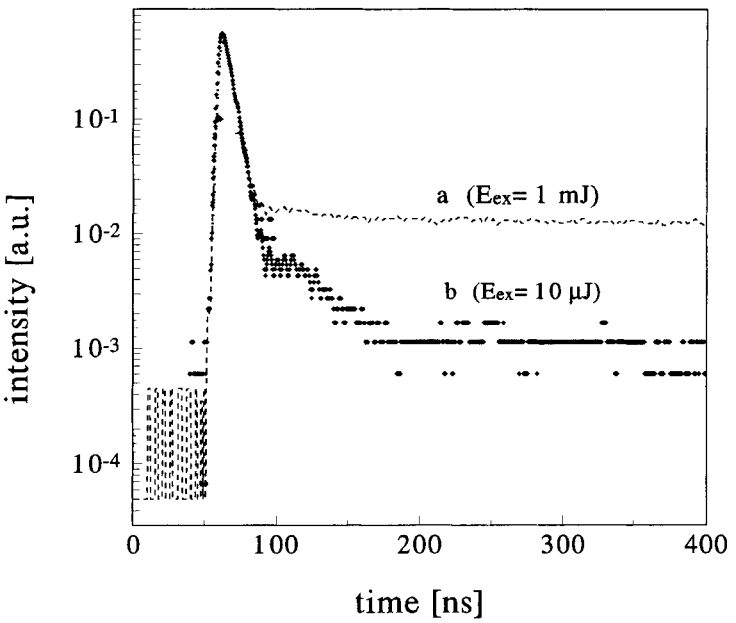

Fig. 8. PWO 1180 PL decay at RT and $\lambda_{em} = 500$ nm excited by the N_2-laser line 337.1 nm. a) $E_{ex} = 1$ mJ, b) 10 μJ

the starting PMT pulses (about 40 kHz in this case). Actually, such processes are clearly demonstrated in the PL decays of Fig. 6, 7. The coefficient α is defined in Fig. 9 to give a quantitative measure of such a "superslow" process amplitude in PWO scintillation decay. The values of α are given for several PWO crystals in Table 1 measured at 400 and 500 nm using interference filters (FWHM about 20 nm) and at a spectrally unresolved mode, too.

To obtain an estimate of the superslow decay component content in the case of γ (511 keV) photon excitation, the slowest processes responsible for the nonzero values of α were considered to be single-exponentially decaying. In other words, the overall decay function is supposed as

$$I(t) = \sum_{i=1}^{3} A_i \exp\left[-t/\tau_i\right] + A_{ss} \exp\left[-t/\tau_{ss}\right], \tag{3}$$

where A_i, τ_i ($i = 1$ to 3) are obtained in a sub-μs time scale (Fig. 9) and A_{ss} and τ_{ss} are the amplitude and decay time of the superslow processes, respectively. The true amplitude A_{ss} is related to the observed quantity I_{ss} in Fig. 9 as follows:

$$A_{ss} = I_{ss}(1 - \exp\left[-t_i/\tau_{ss}\right]), \tag{4}$$

where $1/t_i$ equals to the excitation frequency. Equation (4) can be derived in a simple way from a similar procedure used in [15]. The value of the decay time τ_{ss} was determined from two averaged points (t_1, t_2 in Fig. 9) on the decay curve considering their difference in time, namely

$$\tau_{ss} = \frac{t_1 - t_2 + t_i}{\ln\left(I_2/I_1\right)}. \tag{5}$$

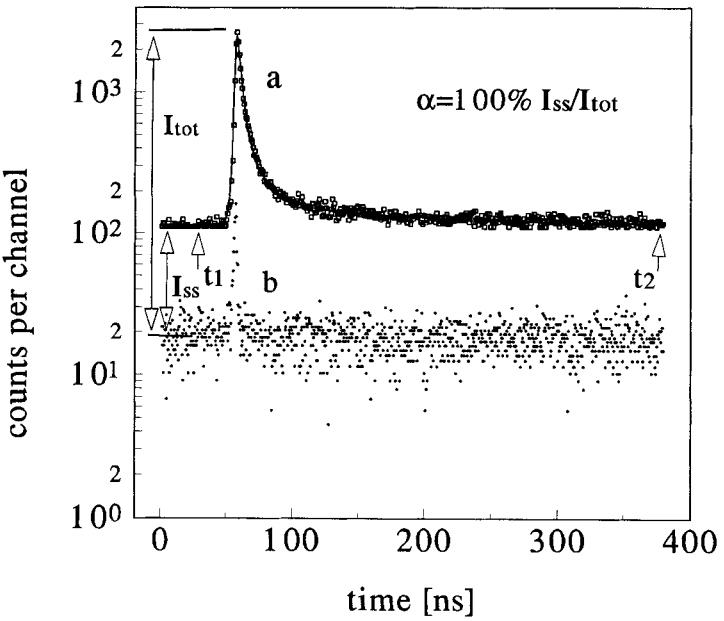

Fig. 9. a) Scintillation decay of PWO 1180, spectrally unresolved, at RT and b) "no crystal" decay measured at the same experimental conditions without the sample. The solid line is the convolution of the instrumental response (derived from "no crystal measurement", see the text) and three exponential approximations with the relative pre-exponential factors A_i and decay times τ_i: $A_1 = 0.521$, $\tau_1 = 3.0$ ns; $A_2 = 0.072$, $\tau_2 = 12.1$ ns; $A_3 = 0.008$, $\tau_3 = 102$ ns

The values of τ_{ss} for all the crystals studied fall into the interval (100, 300) μs, which is of the same order as the values of τ_m calculated from PL decays above. In the framework of this simple approximation, the intensity (light sum) IS_s of superslow processes can be calculated as $IS_s = A_{ss}\tau_{ss}$ and its contribution to the overall decay approximated by (3) is given as

$$IS_s[\%] = \frac{100 A_{ss}\tau_{ss}}{\sum_{i=1}^{i=3} A_i\tau_i + A_{ss}\tau_{ss}} . \tag{6}$$

The calculated values are given in Table 1.

Furthermore, the values of LY are also given in Table 1 for the same crystals using rather small samples of dimensions from $9 \times 9 \times 8$ mm^3 up to $18 \times 18 \times 18$ mm^3.

4. Discussion

As for the general PL characteristics of PWO, most of the measurements presented here (performed on single crystal samples of good quality) confirm the results already published in [1, 2]. Noticeable differences were found only in the case of the temperature dependence of PL decay times, where we measured a more simple monotonically decreasing dependence in contrast to the complex nonmonotonic dependence reported in [1]. The reason might be given by the fact that in [1] the author used also powder samples

obtained by solid state reaction. Different and more complicated defects related to the grain surfaces and interfaces possibly arise in such a case, which can complicate the PL characteristics.

Using the spectra in Fig. 3, it can be derived that while the PWO blue component scintillation intensity is essentially sample independent, huge differences exist in the absolute intensity of the green component, which are determined by the crystal growth technology (green centre concentration obtained). Actually, the difference in the absolute intensity at 500 nm is about two orders of magnitude, when samples 1180 and 1185 are compared. At the same time, comparing the values of α in Table 1 and the spectra in Fig. 3, one can state that clear correlation exists between the absolute green component intensity and the value of α_{unres}. The more intensive the green component is, the higher is the value of α_{unres} calculated. Furthermore, Table 1 shows that superslow processes are mainly related to the green emission component. However, they are always present also in the blue PWO emission where $\alpha_{400\,\text{nm}} \in \langle 0.44,\ 0.94 \rangle\%$.

The existence of nonexponential PL decays down to the ms time scale for both PWO emission components demonstrates the ability of the related emission centres to capture free electrons and holes and serve as radiative recombination centres. The recombination nature of these slower decay processes is further confirmed by their superlinear amplitude dependence on the excitation intensity, Fig. 8. The intensity of the free carrier recombination process is quadratically dependent on the excitation intensity [16], which leads to the relative increase of the recombination-related amplitudes in the decays with respect to the components of the first order. In our case being discussed, the component represented by the decay time τ_1 (Fig. 9) is probably of first order arising at impact excited (not ionized) emission centres, because its value is always very close to the decay time value observed in photoluminescence (Fig. 4). The systematic difference between τ_m calculated for the blue and green PWO emissions indicates the differences in the recombination mechanism. Radiative recombination at the blue emission centres can be considered as the most simple case – free carrier recombination [16a]. An efficient autolocalisation of electrons and/or holes at regular Pb^{2+} ions or WO_4 groups is rather improbable, because even higher intensity of recombination processes is observed at the green emission centres. The latter are of defect origin having concentrations at least two to three orders of magnitude lower comparing to the regular lattice sites. This means that efficient transport of electrons and holes to the green emission centres takes place and the carriers become deeply localized only here. Different mechanisms of recombination processes are appropriate in this case, namely recombination of free carriers at lattice defects [16b]. This is further supported by the fact that the thermostimulated luminescence spectrum of PWO is situated in the green spectral region [14] very close to the position of the green photoluminescence component.

The higher intensity of slow recombination processes in the green emission component is possibly further enhanced by the effect demonstrated in the observed departure from the single exponential course of PL green component above 180 K (Fig. 5b at 220 K). This phenomenon might show that there is a nonzero probability of thermal decomposition of the green emission centre in the excited state, which (followed by another free carrier (electron) capture at a later stage and radiative recombination afterwards) increases further the intensity of recombination processes in the decay. The observed effect might also be induced by the observed PWO structure instabilities and the anomalous behaviour at temperatures of 200 to 300 K [17].

Another distinct correlation exists between the values of α and the observed LY of the PWO crystals studied. In fact, an increase of the LY cannot be explained directly by increasing α, superslow processes do not contribute significantly to the LY measured, because the measurement is performed in ac mode. However, the increase of α is always accompanied by the increased intensity of the processes represented by τ_2 and τ_3 in Fig. 9, which contribute to the increase of LY measured. The just mentioned simultaneous increase of α and the processes approximated by τ_2 and τ_3 most probably means that all these characteristics are related to the same process, the recombination of free electrons and holes at the blue and green emission centres. Recombination kinetics thus show temporal dependence in a very wide time scale, namely 10^{-8} to 10^{-1} s. In other words, radiative recombination of free electrons and holes gives a positive contribution to the LY even for a time gate less than 100 ns. However, the slowest components of the same process give rise to the overlap of scintillation responses from many preceding events even at an (excitation) event frequency of several tens of kHz, which is characterized by the coefficient α.

The light sum released in the first 100 ns after excitation and its fraction in the overall photoluminescence intensity ((2), $I_f \doteq 1.5\%$) is determined quite precisely from Fig. 9. However, because of the simple approximation of the superslow component decay course in the scintillation decay the values obtained for IS_s have to be taken with caution. Nevertheless, the estimate shows that probably the major part of the scintillation light in PWO crystals is released at times $t > 200$ to 400 ns at least in the PWO samples with strongly enhanced green emission component.

It is also to note that the values of the coefficient α might be slightly overestimated, because the ^{22}Na radioisotope produces (apart from 511 keV photons) also 1274 keV photons, which are uncorrelated in space to the 511 keV ones. However, this fact does not change any of the conclusions drawn in this paper.

From the physical point of view, the existence of recombination processes in PWO emission can explain its generally nonexponential course through several orders of magnitude in time. The widely used decay curve approximation by a sum of exponentials can be hardly interpreted in the case of PWO. Beside τ_1 (fit in Fig. 9), which is close to the decay time values observed also in PL decay (Fig. 4), there are no excited state levels available to offer appropriate transition dipole moments to justify the existence of several decay times from about 10 ns down to 10 ms obtainable from a multi-exponential approximation of the decay.

5. Conclusion

The correlations among the absolute value of PWO green emission component intensity, the amplitude of superslow processes in the scintillation decay, and related values of the LY were put into evidence. The existence of recombination processes in PWO decay was proved as a general phenomenon in this material, which shows temporal dependence down to the ms time scale. These processes are present mainly in the green PWO emission, however, the blue emission centres are also taking part in the radiative free carrier recombination, even if the nature of recombination processes is probably different from the situation in the green PWO emission component. The calculated estimates allow to conclude that at room temperature the major part of the PWO light is released at times greater than some hundreds of ns both in the photoluminescence and scintillation decays in the case of PWO crystals with a strongly enhanced green emission component.

Acknowledgements This work was performed in the framework of Crystal Clear Collaboration. One of the authors (K.N.) undertook this work with the support of the Deutsche Forschungsgemeinschaft in the Laboratories of the Institute for Crystal Growth in Berlin, the work of M.N. was partially supported by the ICTP Programme for Training and Research in Italian Laboratories, Trieste, Italy. Partial support from EC Network Grant CIPD 940037 is also gratefully acknowledged.

References

[1] W. van Loo, phys. stat. sol. (a) **27**, 565 (1975); **28**, 227 (1975).
[2] J. A. Groenink and G. Blasse, J. Solid State Chem. **32**, 9 (1980).
[3] R. Grasser, E. Pitt, A. Scharmann, and G. Zimmerer, phys. stat. sol. (b) **69**, 359 (1975).
[4] V. G. Barishevski et al., Nuclear Instrum. and Methods **A322**, 231 (1992).
[5] M. Kobayashi, M. Ishii, Y. Usuki, and H. Yahagi, Nuclear Instrum. and Methods **A333**, 429 (1993).
[6] S. Anderson et al. (82 authors of CCC collaboration), Nuclear Instrum. and Methods **A332**, 373 (1993).
[7] P. Lecoq et al., Lead Tungstate Scintillators for LHC EC Calorimetry, ref. 10151, Nuclear Instrum. and Methods **A365**, 291 (1995).
[8] M. Nikl, K. Polak, K. Nitsch, E. Mihokova, P. Lecoq, I. Dafinei, P. Reiche, R. Uecker, and O. Jarolimek, Luminescence and Scintillation of $PbWO_4$ Single Crystals, in: Inorganic Scintillators and Their Applications, ed. by P. Dorenbos and C. W. van Eijk, Delft University Press, 1995 (p. 257), Proc. SCINT'95, Aug. 28 to Sep. 1, 1995, Delft (The Netherlands).
[9] M. Kobayashi, M. Ishii, K. Harada, Y. Usuki, H. Okuno, H. Shimizu, and T. Yazawa, Further Studies on Excitation–Emission Spectra, Radiation Damages, and Mechanical Properties of $PbWO_4$, ibid. (p. 286).
[10] K. Polák, D. J. S. Birch, and M. Nikl, phys. stat. sol. (b) **145**, 741 (1988).
[11] L. M. Bollinger and G. E. Thomas, Rev. Sci. Instrum. **32**, 1044 (1961).
[12] K. Nitsch, M. Nikl, S. Ganschow, P. Reiche, and R. Uecker, The Growth of $PbWO_4$ Single Crystal Scintillator, accepted in J. Crystal Growth.
[13] Z. W. Yin and Z. L. Xue, Recent Progress on the R & D of Large Size CsI (Tl) and $PbWO_4$ Crystals, see [8] (p. 490).
[14] E. Auffray, I. Dafinei, P. Lecoq, and M. Schneegans, Radiat. Eff. Def. **135**, 343 (1995).
[15] T. Matsumoto, T. Kawata, A. Miyamoto, and K. Kan'no, J. Phys. Japan **61**, 4229 (1992).
[16] J. S. Blakemore, Semiconductor Statistics, a) Chap. 5, b) Chap. 7, Dover Publ., Inc., New York 1987.
[17] N. V. Klassen et al., Relation between Crystalline Structure and Properties of Scintillators, see [8] (p. 475).